Published in final edited form as:
Brain Res. 2010 November 11; 1360: 77–88. doi:10.1016/j.brainres.2010.08.102.

Activation of reciprocal pathways between arcuate nucleus and ventrolateral periaqueductal gray during electroacupuncture: *involvement of VGLUT3*

Zhi-Ling Guo and **John C. Longhurst**[a]
[a]Department of Medicine and Susan-Samueli Center for Integrative Medicine, School of Medicine, University of California, Irvine, Irvine, CA 92697, USA

Abstract

Electroacupuncture (EA) at the Jianshi-Neiguan acupoints (P5-P6, overlying the median nerve) attenuates sympathoexcitatory responses through activation of the arcuate nucleus (ARC) and ventrolateral periaqueductal gray (vlPAG). Activation of the ARC or vlPAG respectively leads to neuronal excitation of the both nuclei during EA. However, direct projections between these two nuclei that could participate in central neural processing during EA have not been identified. The vesicular glutamate transporter 3 (VGLUT3) marks glutamatergic neurons. Thus, the present study evaluated direct neuronal projections between the ARC and vlPAG during EA, focusing on neurons containing VGLUT3. Seven to ten days after unilateral microinjection of a rodamine-conjugated microsphere retrograde tracer (100 nl) into the vlPAG or ARC, rats were subjected to EA or served as a sham-operated control. Low frequency (2 Hz) EA was performed bilaterally for 30 min at the P5-P6 acupoints. Perikarya containing the microsphere tracer were found in the ARC and vlPAG of both groups. Compared to controls (needle placement without electrical stimulation), c-Fos immunoreactivity and neurons double-labeled with c-Fos, an immediate early gene and the tracer were increased significantly in the ARC and vlPAG of EA-treated rats (both $P<0.01$). Moreover, some neurons were triple-labeled with c-Fos, the retrograde tracer and VGLUT3 in the two nuclei following EA stimulation ($P<0.01$, both nuclei). These results suggest that direct reciprocal projections between the ARC and vlPAG are available to participate in prolonged modulation by EA of sympathetic activity and that VGLUT3-containing neurons are an important neuronal phenotype involved in this process.

Keywords

acupuncture; arcuate nucleus; c-Fos; neural pathways; periaqueductal gray; vesicular glutamate transporter

1. Introduction

Acupuncture has been used for several centuries by physicians in eastern countries to treat a number of diseases, and increasingly is being accepted as an integrative medical therapy in

Address for correspondence: Zhi-Ling Guo, M.D., Ph.D., Department of Medicine, C240 Medical Science 1, University of California, Irvine, Irvine, California 92697-4075, U.S.A., Tel: 949-824-8161, Fax: 949-824-2200, zguo@uci.edu.

the West. The Jianshi-Neiguan acupoints (P5-P6, overlying the median nerve) are commonly used to manage cardiovascular disorders (Li et al., 1998). However, the mechanisms determining its actions are largely unknown. Our studies have shown that electroacupuncture (EA) at the P5-P6 acupoints along the forearm reduces sympathoexcitatory responses, in part, through activation of cells in the hypothalamic arcuate nucleus (ARC) and ventrolateral periaqueductal gray (vlPAG) within the midbrain (Li et al., 2006;Tjen-A-Looi SC et al., 2006). Activation of these nuclei during EA ultimately leads to inhibition of sympathetic premotor neurons in the rostral ventral lateral medulla (rVLM) and attenuation of reflex increases in blood pressure (Li et al., 2009;Tjen-A-Looi SC et al., 2006;Tjen-A-Looi SC et al., 2007). We also have found that activation of the ARC or vlPAG during EA leads to excitation of neurons in the vlPAG or ARC, respectively, suggesting the presence of an excitatory neural circuit between these two nuclei (Li et al., 2010). Although anatomical evidence has shown direct projections between these two nuclei (Sim and Joseph, 1991;Reichling and Basbaum, 1991), it is unclear if these direct pathways participate in the EA-evoked reciprocal activation.

Glutamate is an important and ubiquitous excitatory neurotransmitter in the brain. Moreover, glutamatergic neurons and receptors are present in the ARC and vlPAG (Eyigor et al., 2001;Ishide et al., 2005;Guo and Longhurst, 2007;Kiss et al., 2005). In this regard, we have noted that ARC neurons activated by EA at the P5-P6 acupoints, as identified by their expression of c-Fos, contain vesicular glutamate transporter 3 (VGLUT3), a marker for glutamate (Guo and Longhurst, 2007;Guo et al., 2004;Noh et al., 2010;Seal et al., 2009). However, it is unknown if ARC neurons containing VGLUT3 activated by EA directly project to the vlPAG. Furthermore, there is no information on the activation of VGLUT3-containing neurons in the vlPAG during EA, or their projections to the ARC.

As such, the specific aim of the present study was to determine if EA at the P5– P6 acupoints activates reciprocal projections between the ARC and vlPAG, specifically focusing on neurons containing VGLUT3. We hypothesized that EA activates reciprocal ARC-vlPAG VGLUT3-related pathways.

2. Results

2.1. ARC and vlPAG neurons co-labeled with retrograde tracer and c-Fos

Seven animals were eliminated from this study since the sites for microinjection were found to be outside the ARC or vlPAG. Twenty-one rats were included in this study. As described previously (Li et al., 2010), we consistently observed that neurons labeled with the microsphere tracer were distributed rostrally and caudally throughout the ARC when the tracer was deposited in the vlPAG in 11 rats subjected to EA and in controls. Similarly, microspheres injected into the ARC in 10 other rats from EA-treated and controls, were observed to be present throughout the vlPAG at multiple rostral-caudal levels. Approximately two-thirds of the neurons labeled with microspheres in the ARC and vlPAG were found to be located ipsilateral to the injected site when the retrograde tracer was administered into the opposite nucleus. Distribution patterns of the tracer-labeled neurons in the ARC and vlPAG were similar in EA-treated and control rats.

Like our findings in cats (Guo et al., 2004;Guo and Longhurst, 2007), we detected more neurons with Fos immunoreactivity in EA-treated rats than in controls in the ARC and vlPAG, especially in the caudal region of the vlPAG. Importantly, we also observed that Fos nuclei in the ARC and vlPAG co-localized with neurons labeled with the retrograde tracer that had originated from the opposite nucleus (Figs 2 and 3). These double-labeled neurons were found significantly more frequently in EA-treated rats than in controls ($p<0.05$). However, there were similar numbers of neurons labeled with the retrograde tracer in the

ARC and vlPAG of both groups (Figs 4 and 5, Tables 1 and 2). Photomicrographs in Figures 2 and 3 show examples of confocal images displaying a neuron double-labeled with c-Fos and the microsphere tracer in the ARC and vlPAG of EA-treated rats.

2.2. ARC and vlPAG neurons co-labeled with retrograde tracer + c-Fos + VGLUT3

As we found in the cat (Guo and Longhurst, 2007), neurons labeled with VGLUT3 were located in the ARC of rats. We also observed VGLUT3-labeling in the vlPAG (Fig. 6). The patterns of VGLUT3-labeling in the ARC and vlPAG were similar in EA-treated and control rats (Tables 1 and 2). We found that many VGLUT3-labeled neurons co-localized with the retrograde tracer in the ARC as well as in the vlPAG (Tables 1 and 2).

Co-localization of Fos nuclei with the retrograde tracer and VGLUT3 was observed frequently in the ARC and vlPAG in EA-treated rats, but only rarely in control animals (Figs 4 and 5). There were significant differences between two groups (Tables 1 and 2). Figures 7 and 8 demonstrate confocal images of neurons triple-labeled with c-Fos, retrogradely transported microspheres and VGLUT3 in the ARC and vlPAG of rats that had been subjected to EA.

3. Discussion

Stimulation of acupuncture points, or acupoints, located on the skin along pathways called meridians, assists in treatment of a number of cardiovascular diseases including hypertension, arrhythmias and conditions associated with myocardial ischemia (Li et al., 1998;Richter et al., 1991;Lujan HL et al., 2007;Flachskampf FA et al., 2007). Previously, we demonstrated that EA at the P5–P6 acupoints in animals significantly reduces the extent of myocardial ischemia (Chao et al., 1999;Li et al., 1998). EA also modulates blood pressure elevations that result from sympathoexcitation during visceral reflex stimulation (Moazzami A et al., 2010;Li et al., 2002;Tjen-A-Looi SC et al., 2006). These responses are associated with EA modulation of sympathetic nerve activity through its action on a number of brain nuclei. In this respect, our studies have shown that both the ARC and vlPAG receive excitatory input from somatic nerves underlying P5–P6 acupoints, which profoundly influence reflex sympathoexcitatory responses (Li et al., 2006;Tjen-A-Looi SC et al., 2006). Furthermore, our recent electrophysiological studies suggest the potential for reciprocal interactions between the ARC and vlPAG during EA, which influence visceral excitatory input for prolonged periods of time far outlasting the actual EA stimulus (Li et al., 2010). To more thoroughly investigate these interactions, the present study evaluated interactions between these nuclei using a combined c-Fos immunohistochemistry and track tracing approach incorporating retrograde labeling with colored microspheres (Kantzides et al., 2005). Data from this study provide the first evidence for direct projection of neurons activated by median nerve stimulation at the P5–P6 acupoints (c-Fos positive cells) from the ARC to the vlPAG and reciprocally from the vlPAG to the ARC. Some of these ARC and vlPAG neurons were demonstrated to be glutamatergic, as identified by their expression of VGLUT3. These data provide firm support for direct reciprocal ARC-vlPAG connections that can be activated by somatic nerve stimulation during acupuncture.

The ARC serves a number of functions linking pain and other sensory inputs as well as vegetative homoeostatic and autonomic responses (Chronwall, 1985). The vlPAG, especially its caudal extension, has been implicated in cardiovascular regulation as part of a non-nociceptive defense reaction (Carrive et al., 1987;Hilton and Redfern, 1986). This region also provides analgesia with alerting (including noxious) stimuli,(Morgan and Liebeskind, 1987). Cells in the vlPAG that project to the rVLM transmit information related to cardiovascular and pain modulation (Carrive et al., 1987;Farkas et al., 1998;Punnen et al., 1984;VanBockstaele et al., 1989). Moreover, anatomical and physiological studies from our

laboratory suggest that the ARC and vlPAG are activated during EA and are involved in acupuncture-related neural regulation (Guo et al., 2004;Guo and Longhurst, 2007;Li et al., 2006;Tjen-A-Looi SC et al., 2006).

Previously, retrograde and anterograde tracing studies have suggested direct connections between the ARC and the vlPAG. In this regard, in the vlPAG, Sim and Joseph observed neural fibers originating from the ARC, while Reichling and Basbaum found cells labeled with the retrograde tracer that had been injected in the ARC (Sim and Joseph, 1991;Reichling and Basbaum, 1991). Consistent with these earlier findings, we recently demonstrated the presence of cells containing retrograde microspheres in the ARC and vlPAG after they were injected into the opposite nucleus, further supporting the possibility of direct reciprocal projections between these two nuclei (Li et al., 2010). Although our earlier study did not determine if these direct reciprocal connections were activated by EA, the present study utilizing c-Fos immunocytochemistry demonstrates that many of the neurons forming these reciprocal connections are activated during 30 min of low frequency, low intensity EA.

c-Fos, an immediate early gene, is rapidly but transiently expressed following cellular stimulation (<5 h) and serves as a marker to identify neuronal activation (Guo et al., 2002). We took care to minimize the expression of c-Fos in the brain induced by non-specific stimuli, including anesthesia and surgical procedures as we described in the Methods. Thus, the survival surgical procedure for microinjection of retrograde tracer was conducted at least seven days prior to EA stimulation. In addition, rats were allowed to stable for 4 h after acute minor surgery, before treatment with EA. Most importantly, EA-treated and sham-operated controls were performed with only one difference between control and EA, i.e., electrical stimulation of acupuncture needles at P5–P6, which was not applied to the control group. Thus, compared to controls, the pattern of increased c-Fos in the EA-treated rat was caused exclusively by electrical stimulation of needles placed in the P5–P6 acupoints rather than by other non-specific stimuli. Like many other studies using c-Fos immunohistological staining, we previously have demonstrated that EA activates neurons in the ARC and vlPAG by evaluating Fos expression (Guo et al., 2004;Guo and Longhurst, 2007). Similar to these observations in cats, the current study documents that EA induces c-Fos expression in the ARC and vlPAG of rats. Taken together, the past and present studies show that neurons in the ARC and vlPAG are activated by EA and that they project directly to the other nucleus.

Glutamate is a ubiquitous excitatory neurotransmitter in the brain. This excitatory amino acid and its receptors have been identified in the ARC and vlPAG (Albin et al., 1990;Eyigor et al., 2001;Ishide et al., 2005;Guo and Longhurst, 2007;Kiss et al., 2005). Vesicular glutamate transporters (VGLUTs) specifically transport glutamate into vesicles of neurons, and thus offer a unique marker to distinctively identify neurons that use glutamate as a neurotransmitter (Fremeau et al., 2002). While the VGLUT1 and VGLUT2 antisera mainly label nerve fibers, the staining pattern of both cell bodies and nerve fibers is obtained with VGLUT3 antiserum (Guo et al., 2005;Guo and Longhurst, 2006). Therefore, in this study, we evaluated co-localization of VGLUT3 with perikarya containing the tracer and c-Fos nuclei following EA. Similar to VGLUT1 and VGLUT2, VGLUT3 is present in some neurons that contain other neurotransmitters like gamma-aminobutyric acid (GABA), suggesting the potential for co-release of glutamate with other neural substance(s) (Fattorini et al., 2009;Boulland et al., 2009;Noh et al., 2010). Although there has been discussion about the specificity of VGLUT3 for glutamatergic neurons, VGLUT3 is considered by many to be a useful marker for neurons that contain glutamate (Guo and Longhurst, 2007;Fremeau et al., 2002;Noh et al., 2010;Seal et al., 2009;Gritti et al., 2006). In this respect, Gritti et al. have shown that almost all (96–100%) VGLUT3-labeled neurons are positively stained for phosphate-activated glutaminase (pGlu), an enzyme that synthesizes

glutamate from glutamine (Gritti et al., 2006). Moreover, VGLUT3 is closely associated with calcium-dependent release of glutamate from astrocytes (Ni and Parpura, 2009). As such, the VGLUT3 labeling represents a valuable way to visualize glutamatergic neurons in the brain.

In this study, we initially found that VGLUT3 co-localized with neurons containing the retrograde tracer in the ARC and vlPAG that had been injected into the opposite nucleus, suggesting reciprocal glutamatergic projections between the ARC and vlPAG. Additionally, we noted co-localization of VGLUT3 and the retrograde tracer in some neurons that were activated by EA, identified by their expression of c-Fos. On the other hand, we noticed that more than half of neurons co-labeled with retrograde tracer and c-Fos in the ARC and vlPAG are glutamatergic. These data suggest that glutamate only partially but significantly contributes to processing activation of ARC-vlPAG reciprocal pathways during EA stimulation of somatic afferents. Thus, the results from this study support our recent physiological and pharmacological findings of glutamatergic neural circuits between the ARC and vlPAG that mediate the prolonged influence of EA on cardiovascular function (Li et al., 2006).

While we believe that glutamate plays a role in excitation of ARC-vlPAG reciprocal pathways during EA, we also realize that there likely is contribution from other neurotransmitters to this process since not all of retrogradely labeled neurons activated by EA in the ARC and vlPAG are glutamatergic. In other regions of the brain, VGLUT3 exists in neurons that contain transmitters, such as GABA, acetylcholine or serotonin (Gritti et al., 2006;Stornetta et al., 2005). In this regard, we have shown that disinhibition of GABAergic neurons through endocannabinioid CB1 receptor stimulation presynaptically in the vlPAG is important in vlPAG-rVLM excitation during EA ((Fu and Longhurst, 2009;Tjen-A-Looi et al., 2009). Also, acetylcholine in the arcuate participates in vlPAG-ARC reciprocal actiation (Li et al., 2010). Although acetylcholine is important excitatory neurotransmitter in the ARC, with respect to the excitation of the vlPAG, the converse (cholinergic vlPAG→ARC) is not an important mechanism that is operative during EA and it is not known, if, in addition to glutamate, other neurotransmitters like GABA are important in the vlPAG-ARC pathway. Thus, it is likely that other neurotransmitters in addition to glutamate participate in processing somatic information through the ARC and vlPAG during EA.

In summary, the ARC and vlPAG are important hypothalamic and midbrain nuclei that process information from somatic afferents during EA. Results from the present study suggest that direct reciprocal projections between the ARC and vlPAG have the potential to contribute to the prolonged EA effects through activation of glutamatergic neurons. These excitatory neural pathways have the capacity to facilitate and prolong the response of ARC and vlPAG neurons receiving input from the somatic nervous system.

4. Experimental Procedures

4.1. Microinjection of retrograde tracer into vlPAG and ARC

All procedures were carried out in accordance with the Society for Neuroscience and the National Institutes of Health guidelines. The minimum possible number of rats (n=28) was used to obtain reproducible and statistically significant results in this study. In addition, every effort was made to minimize any discomfort and suffering. Surgical and experimental protocols were approved by the Animal Use and Care Committee at the University of California, Irvine. Adult male Sprague-Dawley rats (350–500 g) were used to microinject a retrogradely transported microsphere tracer into the ARC or vlPAG to evaluate for direct projections between these two nuclei, as described in detail in our previous studies (Li et al., 2009;Li et al., 2010) . Briefly, a mixture of ketamine/xylazine (80/12 mg/ml, Sigma) was

used to induce (0.3–0.4 ml, i.m) and maintain (0.1–0.2 ml, i.m) anesthesia in the animals. Body temperature was monitored with a rectal probe and was maintained at 37°C. Heart rate and oxygen saturation were monitored using a pulse oximeter (Nonin Medical, Inc. Plymouth, MN USA). Following induction, rats were positioned in a stereotaxic apparatus (David Kopf Instruments). A one inch incision was made to expose the skull. A burr hole (4 mm diameter) was made in the bone so that a glass micropipette could be inserted using the following coordinates: for vlPAG injection, 7.0 – 8.8 mm caudal from the bregma; 0.5 – 1.2 mm from the midline and 6.0 – 6.8 mm deep from the dural surface; for ARC injection, 1.8 – 3.6 mm caudal from the bregma; 0.3 – 0.5 mm from the midline and 8.8 – 9.6 mm deep from the dural surface. The retrogradely transported tracer, rhodamine-labeled fluorescent microspheres in suspension (0.04 μm, Molecular Probes, Eugene, OR), was injected unilaterally into the vlPAG or ARC through the glass micropipette (100 nl). The wound was sutured shut. Microspheres were transported during a 7–10 day recovery and maintenance period.

Terminal procedures occurred 7 to 10 days after administration of the retrograde tracer. Rats were re-anesthetized with ketamine/xylazine, as described above. An adequate depth of anesthesia was maintained as judged by stability of respiration, blood pressure and heart rate and the lack of a withdrawal response to toe pinch. A femoral artery and vein were cannulated for measuring arterial blood pressure (BP, Statham P 23 ID, Oxnard, CA, USA) and administering drugs and fluids. Heart rate (HR) was derived from the arterial pressure pulse with a biotach (Gould Instrument, Cleveland, OH, USA). The animal was ventilated artificially through a cuffed endotracheal tube after incubation. Arterial blood gases and pH were monitored with a blood gas analyzer (Radiometer, Inc., Model ABL-3, Westlake, OH, USA). They were kept within normal limits (PO_2, 100–150 mm Hg; PCO_2, 28–35 mm Hg; pH, 7.35–7.45) by adjusting the volume and/or the ventilation rate, enriching the inspired O_2 supply and administration of 1 M $NaHCO_3$. Body temperature was maintained at 36–38 °C by a water heating pad and a heat lamp.

After the rats were stabilized for 4 h following surgical preparation, pairs of stainless steel, 38-gauge (0.18 mm × 13 mm) acupuncture needles were inserted bilaterally at the P5–P6 acupoints, overlying the median nerves. The P5–P6 acupoints on both forelimbs of small animals are analogous to those in humans (Hua, 1994). The needles were connected to a constant current stimulator with a stimulus isolation unit and stimulator (Grass, model S88, W. Warwick, RI, USA).

4.2. Experimental protocols

Rats subjected for microinjection of the retrograde tracer into the ARC or vlPAG were divided randomly into an EA-treated group and a sham-operated control group. As in our previous studies (Guo and Longhurst, 2007;Li et al., 2002), low-frequency, low current EA (0.5 ms pulses, 2 Hz, 2–5 V, 1–4 mA) was administered for 30 min in the present investigation. This stimulation was sufficient to produce moderate, repeated paw flexion in each forelimb, which confirmed stimulation of the median nerve (Li et al., 1998;Li et al., 2002;Tjen-A-Looi et al., 2007). Each set of electrodes was stimulated separately so that current did not flow from one location to the contralateral side. In control animals, acupuncture needles were put into the P5–P6 acupoints for 30 min but were not stimulated electrically following insertion. We have demonstrated that this control does not evoke input to the rVLM or modulate sympathetic reflexes and serves as an adequate control for EA (Zhou et al., 2005;Tjen-A-Looi SC et al., 2004;Tjen-A-Looi SC et al., 2007;Li et al., 2009). There were no changes in basal BP and HR during EA or sham-operated stimulation in both EA and control groups as we have noted previously (Zhou et al., 2007;Li et al., 2004;Crisostomo et al., 2005).

4.3. Immunohistochemical staining

4.3.1. Tissue preparation—As described in our previous studies (Guo and Longhurst, 2003;Li et al., 2009), 90 min after termination of EA or the control, deep anesthesia was induced by another larger dose of the ketamine/xylazine (0.5–0.7 ml, i.m.). Transcardial perfusion was performed using 500 ml of 0.9% saline solution followed by 500 ml of 4% paraformaldehyde in 0.1 M phosphate buffer (pH 7.4). The diencephalon and mesencephalon were harvested and sliced in coronal sections (30 μm) using a cryostat microtome (Leica CM1850 Heidelberger Strasse, Nussloch, Germany). Brain sections were placed serially in cold cryoprotectant solution (Chan and Sawchenko, 1994) and were used for immunohistochemical labeling as described below and identifying sites of microsphere tracer injection. Animals were included for immunohistochemical staining and data analysis if the site for microinjection was found to be in the ARC or vlPAG, as samples shown in the figure 1 indicate. In this study, free-floating sections were used for labeling.

4.3.2. Immunohistochemistry

Single c-Fos or VGLUT3 immunohistochemical labeling: After washing for 30 min (10 min × 3 times) in phosphate-buffered saline containing 0.3% Triton X-100 (PBST; pH = 7.4), brain sections were placed for 1 h in 1% normal donkey serum (Jackson Immunoresearch Laboratories, West Grove, PA). The sections were incubated with a primary polyclonal rabbit anti-Fos antibody (1:2,000 dilution, Oncogene research product, Calbiochem, San Diego, CA, USA) or a primary guinea-pig polyclonal anti-VGLUT3 antibody (1:500 dilutions, Chemicon International, Temecula, CA) at 4°C for 48 h. The tissues subsequently were rinsed three times (10 min for each rinse) in PBST and incubated with a fluorescein-conjugated donkey anti-rabbit or anti-guinea pig antibody (1:200; Jackson Immunoresearch Laboratories) for 24 h at 4°C. Each section was mounted on a slide and was air dried. The slides were coverslipped using mounting medium (Vector Laboratories, Burlingame, CA). Immunohistochemical control studies were performed by omission of the primary or secondary antibodies. No labeling was detected under these conditions.

Double-fluorescent immunohistochemical labeling for c-Fos + VGLUT3: The staining procedures were similar to those used for single-fluorescent immunohistochemical labeling described above. Briefly, after treatment with PBST and 1% normal donkey serum, brain tissues were incubated with two primary antibodies, including a rabbit polyclonal anti-c-Fos antibody (1:2,000 dilution) and a guinea-pig anti-VGLUT3 antibody (1:500 dilution) for 48 h at 4°C. Sections then were incubated with a fluorescein-conjugated donkey anti-rabbit antibody and a coumarin-conjugated donkey anti-guinea-pig antibody (all 1:100; Jackson Immunoresearch Laboratories) at 4°C for 24 h. The sections were mounted on slides and coverslipped with mounting medium (Vector Laboratories). In the immunohistochemical control studies, no stain was detected when the primary or secondary antibody was omitted.

4.3.3. Data analysis—Brain sections were scanned and examined with a standard fluorescent microscope (Nikon, E400, Melville, NY). Three epifluorescence filters (B-2A, G-2A, or UV-2A) equipped in a fluorescent microscope were used to identify single stains appearing as green (fluorescein), red (rhodamine), or blue (coumarin) in brain sections. Sections containing the ARC or vlPAG were identified according to their best matched standard stereotaxic plane, as shown in Paxinos and Watson's atlas for the rat (Paxinos and Watson, 2005).

After examination with the fluorescent microscope, selected sections were further evaluated with a laser scanning confocal microscope (Zeiss LSM 510, Meta System, Thornwood, NY) to confirm co-localization of two or three labels. This apparatus was equipped with Argon and HeNe lasers and allowed operation of multiple channels. Lasers of 488- and 543-nm

wavelengths were used to excite fluorescein (green) and rhodamine (red), respectively. A 790-nm laser was applied for two-photon excitation of coumarin (blue). Digital fluorescent images were captured and analyzed with software (Zeiss LSM) provided with the confocal microscope. Each confocal section analyzed was limited to 0.5 μm thickness in the *Z*-plane. Images containing more than two colors in the same plane were merged to reveal the relationship between two and/or three labels (see Fig. 8). Single-, double- and triple-labeled neurons were evaluated.

The numbers of single-, double- and triple-labeled cells in the same section were counted in each animal. The average number of labeled neurons derived from the three representative levels taken from the rostro-caudal extension of the ARC or vlPAG (Figs 3 and 4) was used to represent the number of neurons per section for statistical analysis (Guo and Longhurst, 2003;Guo et al., 2005).

4.3.4. Statistical analysis—Data are expressed as means ± SE. All statistical analyses were conducted with statistical software (SigmaStat, Version 3.0, Jandel Scientific Software, San Rafael, CA, USA). The Kolmogorov–Smirnoff test was used to determine if data were normally distributed. Comparisons between two groups were analyzed with the Student's *t*-test or Mann–Whitney Rank Sum Test. Values were considered to be significantly different when $P<0.05$.

Research Highlights

Acupuncture activates arcuate nucleus and ventrolateral periaqueductal gray.

Neurons that directly project between these two nuclei are activated by acupuncture.

Some of these activated neurons express vesicular glutamate transporter 3.

Glutamate may excite reciprocal pathways between these two nuclei during acupuncture.

Abbreviations

ARC	Arcuate nucleus
AQ	Aqueduct
EA	Electroacupuncture
GABA	Gamma-aminobutyric acid
P5-P6	Jianshi-Neiguan acupoints
PBST	Phosphate buffered saline containing Triton X-100
rVLM	Rostral ventrolateral medulla
V3	Third ventricle
vlPAG	Ventrolateral periaqueductal gray
VGLUT3	Vesicular glutamate transporter 3

Acknowledgments

We are gratefully thankful to Yu Liu, B.S. and Jesse Ho, B.S. for their technical assistance.

This study was supported by National Heart, Lung, and Blood Institute Grants, HL-072125 and HL-63313.

Reference List

Albin RL, Makowiec RL, Hollingsworth Z, Dure LS, Penney JB, Young AB. Excitatory amino acid binding sites in the periaqueductal gray of the rat. Neurosci Lett. 1990; 118:112–115. [PubMed: 2175406]

Boulland JL, Jenstad M, Boekel AJ, Wouterlood FG, Edwards RH, Storm-Mathisen J, Chaudhry FA. Vesicular glutamate and GABA transporters sort to distinct sets of vesicles in a population of presynaptic terminals. Cereb Cortex. 2009; 19:241–248. [PubMed: 18502731]

Carrive P, Dampney RAL, Bandler R. Excitation of neurones in a restricted portion of the midbrain periaqueductal grey elicits both behavioural and cardiovascular components of the defence reaction in the unanaesthetised decerebrate cat. Neurosci Lett. 1987; 81:273–278. [PubMed: 3431744]

Chan RKW, Sawchenko PE. Spatially and temporally differentiated patterns of c-Fos expression in brainstem catecholaminergic cell groups induced by cardiovascular challenges in the rat. J Comp Neurol. 1994; 348:433–460. [PubMed: 7844257]

Chao DM, Shen LL, Tjen-A-Looi S, Pitsillides KF, Li P, Longhurst JC. Naloxone reverses inhibitory effect of electroacupuncture on sympathetic cardiovascular reflex responses. Am J Physiol. 1999; 276:H2127–H2134. [PubMed: 10362696]

Chronwall B. Anatomy and physiology of the neuroendocrine arcuate nucleus. Peptides. 1985; 6:1–11. [PubMed: 2417205]

Crisostomo M, Li P, Tjen-A-Looi SC, Longhurst JC. Nociceptin in rVLM mediates electroacupuncture inhibition of cardiovascular reflex excitatory response in rats. J Appl Physiol. 2005; 98:2056–2063. [PubMed: 15649868]

Eyigor O, Centers A, Jennes L. Distribution of ionotropic glutamate receptor subunit mRNAs in the rat hypothalamus. J Comp Neurol. 2001; 434:101–124. [PubMed: 11329132]

Farkas E, Jansen ASP, Loewy AD. Periaqueductal gray matter input to cardiac-related sympathetic premotor neurons. Brain Res. 1998; 792:179–192. [PubMed: 9593884]

Fattorini G, Verderio C, Melone M, Giovedi S, Benfenati F, Matteoli M, Conti F. VGLUT1 and VGAT are sorted to the same population of synaptic vesicles in subsets of cortical axon terminals. J Neurochem. 2009; 110:1538–1546. [PubMed: 19627441]

Flachskampf FA, Gallasch J, Gefeller Oe. Randomized trial of acuuncture to lower bldood pressure. Circulation. 2007; 115:3121–3129. [PubMed: 17548730]

Fremeau RJ, Burman J, Qureshi T, Tran C, Proctor J, Johnson J, Zhang H, Sulzer D, Copenhagen D, Storm-Mathisen J, Reimer R, Chaudry F, Edwards R. The identification of vesicular glutamate transporter 3 suggests novel modes of signaling by glutamate. Proc Natl Acad Sci USA. 2002; 99:14488–14493. [PubMed: 12388773]

Fu L-W, Longhurst C. Electroacupuncture Modulates vlPAG Release of GABA through Presynaptic Cannabinoid CB_1 Receptor. Journal of Applied Phsyiology. 2009; 106:1800–1809.

Gritti I, Henny P, Galloni F, Mainville L, Mariotti M, Jones BE. Stereological estimates of the basal forebrain cell population in the rat, including neurons containing choline acetyltransferase, glutamic acid decarboxylase or phosphate-activated glutaminase and colocalizing vesicular glutamate transporters. Neuroscience. 2006; 143:1051–1064. [PubMed: 17084984]

Guo Z-L, Li P, Longhurst J. Central pathways in the pons and midbrain involved in cardiac sympathoexcitatory reflexes in cats. Neuroscience. 2002; 113:433–444.

Guo Z-L, Longhurst J. Activation of nitric oxide-producing neurons in the brain stem during cardiac sympathoexcitatory reflexes in the cat. Neuroscience. 2003; 116:167–178. [PubMed: 12535950]

Guo Z-L, Longhurst J. Responses of neurons containing VGLUT3/nNOS-cGMP in the rVLM to cardiac stimulation. Neuroreport. 2006; 17:255–259. [PubMed: 16462593]

Guo Z-L, Moazzami A, Longhurst J. Electroacupuncture induces c-Fos expression in the rostral ventrolateral medulla and periaqueductal gray in cats: relation to opioid containing neurons. Brain Res. 2004; 1030:103–115. [PubMed: 15567342]

Guo Z-L, Moazzami A, Longhurst J. Stimulation of cardiac sympathetic afferent activates glutamatergic neurons in the parabrachial nucleus: relation to neurons containing nNOS. Brain Res. 2005; 1053:36–48.

Guo Z, Longhurst J. Expression of c-Fos in arcuate nucleus induced by electroacupuncture: Relations to neurons containing opioids and glutamate. Brain Res. 2007; 1166:65–76. [PubMed: 17662967]

Hilton SM, Redfern WS. A search for brain stem cell groups integrating the defence reaction in the rat. J Physiol (Lond). 1986; 378:213–228. [PubMed: 3795103]

Hua, XB. Experimental acupuncture. Shanghai, China: Shanghai Science and Technology Publisher; 1994. Acupuncture manual for small animals; p. 269-290.

Ishide T, Amer A, Maher TJ, Ally A. Nitric oxide within periaqueductal gray modulates glutamatergic neurotransmission and cardiovascular responses during mechanical and thermal stimuli. Neurosci Res. 2005; 51:93–103. [PubMed: 15596245]

Kantzides A, Owens NC, De Matteo R, Badoer E. Right atrial stretch activates neurons in autonomic brain regions that project to the rostral ventrolateral medulla in the rat. Neuroscience. 2005; 133:755–786.

Kiss J, Csaba Z, Csaki A, Halasz B. Glutamatergic innervation of neuropeptide Y and pro-opiomelanocortin-containing neurons in the hypothalamic arcuate nucleus of the rat. Eur J Neurosci. 2005; 21:2111–2119. [PubMed: 15869507]

Li P, Ayannusi O, Reed C, Longhurst J. Inhibitory effect of electroacupuncture (EA) on the pressor response induced by exercise stress. Clinical Autonomic Research. 2004; 14:182–188. [PubMed: 15241647]

Li P, Pitsillides K, Rendig S, Pan H-L, Longhurst J. Reversal of reflex-induced myocardial ischemia by median nerve stimulation: a feline model of electroacupuncture. Circulation. 1998; 97:1186–1194. [PubMed: 9537345]

Li P, Rowshan K, Crisostomo M, Tjen-A-Looi S, Longhurst J. Effect of electroacupuncture on pressor reflex during gastric distention. Am J Physiol. 2002; 283:R1335–R1345.

Li P, Tjen-A-Looi SC, Longhurst JC. The arcuate-ventrolateral periaqueductal gray reciprocal circuit in electroacupuncture cardiovascular inhibition. Autonomic Neuroscience: Basic & Clinical. 2010 In Press.

Li P, Tjen-A-Looi S, Guo Z, Fu L-W, Longhurst JC. Long-loop pathways in cardiovascular electroacupuncture responses. Journal of Applied Phsyiology. 2009; 106:620–630.

Li P, Tjen-A-Looi S, Longhurst J. Excitatory projections from arcuate nucleus to ventrolateral periaqueductal gray in electroacupuncture inhibition of cardiovascular reflexes. Am J Physiol. 2006; 209:H2535–H2542.

Lujan HL, Kramer VJ, DiCarlo SE. Electro-acupuncture Decreases the Susceptibility to Ventricular Tachycardia in Conscious Rats by Reducing Cardiac Metabolic Demand. American Journal of Phsyiology - Heart and Circulatory Physiology. 2007

Moazzami A, Tjen-A-Looi SC, Longhurst JC. Serotonergic Projection from Nucleus Raphe Pallidus to Rostral Ventrolateral Medulla Modulates Cardiovascular Reflex Responses during Acupuncture. J Appl Physiol. 2010; 108:1336–1346. [PubMed: 20133441]

Morgan MM, Liebeskind JC. Site specificity in the development of tolerance to stimulation-produced analgesia from the periaqueductal gray matter of the rat. Brain Res. 1987; 425:356–359. [PubMed: 3427436]

Ni Y, Parpura V. Dual regulation of Ca2+-dependent glutamate release from astrocytes: vesicular glutamate transporters and cytosolic glutamate levels. Glia. 2009; 57:1296–1305. [PubMed: 19191347]

Noh J, Seal RP, Garver JA, Edwards RH, Kandler K. Glutamate co-release at GABA/glycinergic synapses is crucial for the refinement of an inhibitory map. Nat Neurosci. 2010; 13:232–238. [PubMed: 20081852]

Paxinos, G.; Watson, C. The Rat Brain in Stereotaxic Coordinates. Academic Press; 2005.

Punnen S, Willette R, Krieger AJ, Sapru HN. Cardiovascular response to injections of enkephalin in the pressor area of the ventrolateral medullla. Neuropharmacology. 1984; 23:939–946. [PubMed: 6090967]

Reichling DB, Basbaum AI. Collateralization of periaqueductal gray neurons to forebrain or diencephalon and to the medullary nucleus raphe magnus in the rat. Neuroscience. 1991; 42:183–200. [PubMed: 1713655]

Richter A, Herlitz J, Hjalmarson A. Effect of acupuncture in patients with angina pectoris. Eur Heart J. 1991; 12:175–178. [PubMed: 2044550]

Seal RP, Wang X, Guan Y, Raja SN, Woodbury CJ, Basbaum AI, Edwards RH. Injury-induced mechanical hypersensitivity requires C-low threshold mechanoreceptors. Nature. 2009; 462:651–655. [PubMed: 19915548]

Sim LJ, Joseph SA. Arcuate nucleus projections to brainstem regions which modulate nociception. J Chem Neuroanat. 1991; 4:97–109. [PubMed: 1711859]

Stornetta RL, Rosin DL, Simmons JR, McQuiston TJ, Vujovic N, Weston MC, Guyenet PG. Coexpression of vesicular glutamate transporter-3 and gamma-aminobutyric acidergic markers in rat rostral medullary raphe and intermediolateral cell column. J Comp Neurol. 2005; 492:477–494. [PubMed: 16228993]

Tjen-A-Looi SC, Li P, Longhurst JC. Role of medullary GABA, opioids, and nociceptin in prolonged inhibition of cardiovascular sympathoexcitatory reflexes during electroacupuncture in cats. Am J Physiol. 2007; 293:H3627–H3635.

Tjen-A-Looi SC, Li P, Longhurst JC. Medullary substrate and differential cardiovascular response during stimulation of specific acupoints. Am J Physiol. 2004; 287:R852–R862.

Tjen-A-Looi SC, Li P, Longhurst JC. Midbrain vlPAG inhibits rVLM cardiovascular sympathoexcitatory responses during acupuncture. Am J Physiol. 2006; 209:H2543–H2553.

Tjen-A-Looi SC, Li P, Longhurst JC. Endocannabinoid/GABA system in vlPAG during electroacupuncture-related cardiovascular responses. 2007:417.12.

Tjen-A-Looi S, Li P, Longhurst C. Processing Cardiovascular Information in the vlPAG during Electroacupuncture in Rats: Roles of Endocannabinoids and GABA. J Appl Physiol. 2009:1793–1799. [PubMed: 19325030]

VanBockstaele EJ, Pieribone VA, Aston-Jones G. Diverse afferents converge on the nucleus paragigantocellularis in the rat ventrolateral medulla: Retrograde and anterograde studies. J Comp Neurol. 1989; 290:561–584. [PubMed: 2482306]

Zhou W, Fu L-W, Guo Z, Longhurst J. Role of glutamate in rostral ventrolateral medulla in acupuncture-related modulation of visceral reflex sympathoexcitation. American Journal of Phsyiology. 2007; 292:H1868–H1875.

Zhou W, Tjen-A-Looi S, Longhurst JC. Brain stem mechanisms underlying acupuncture modality-related modulation of cardiovascular responses in rats. J Appl Physiol. 2005; 99:851–860. [PubMed: 15817715]

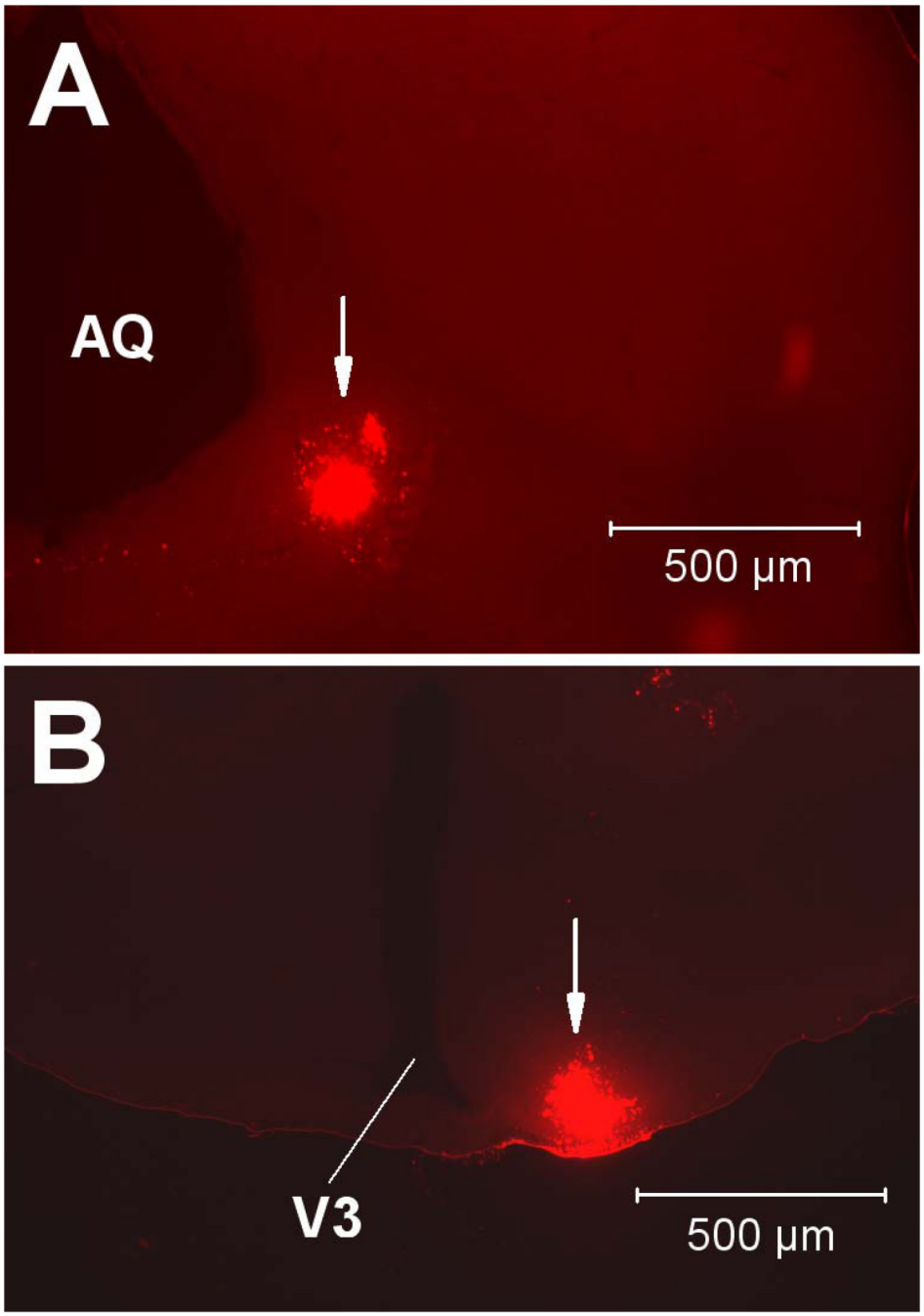

Figure 1.
Fluorescent images showing microinjection sites of the retrograde tracer in vlPAG (*A*, Bregma −8.52 mm) and ARC (*B*, Bregma −3.12 mm), respectively. Arrows in the Panels A and B indicate the injection sites. Scale bars in panels A and B represent 500 μm. AQ, aqueduct; V3, third ventricle.

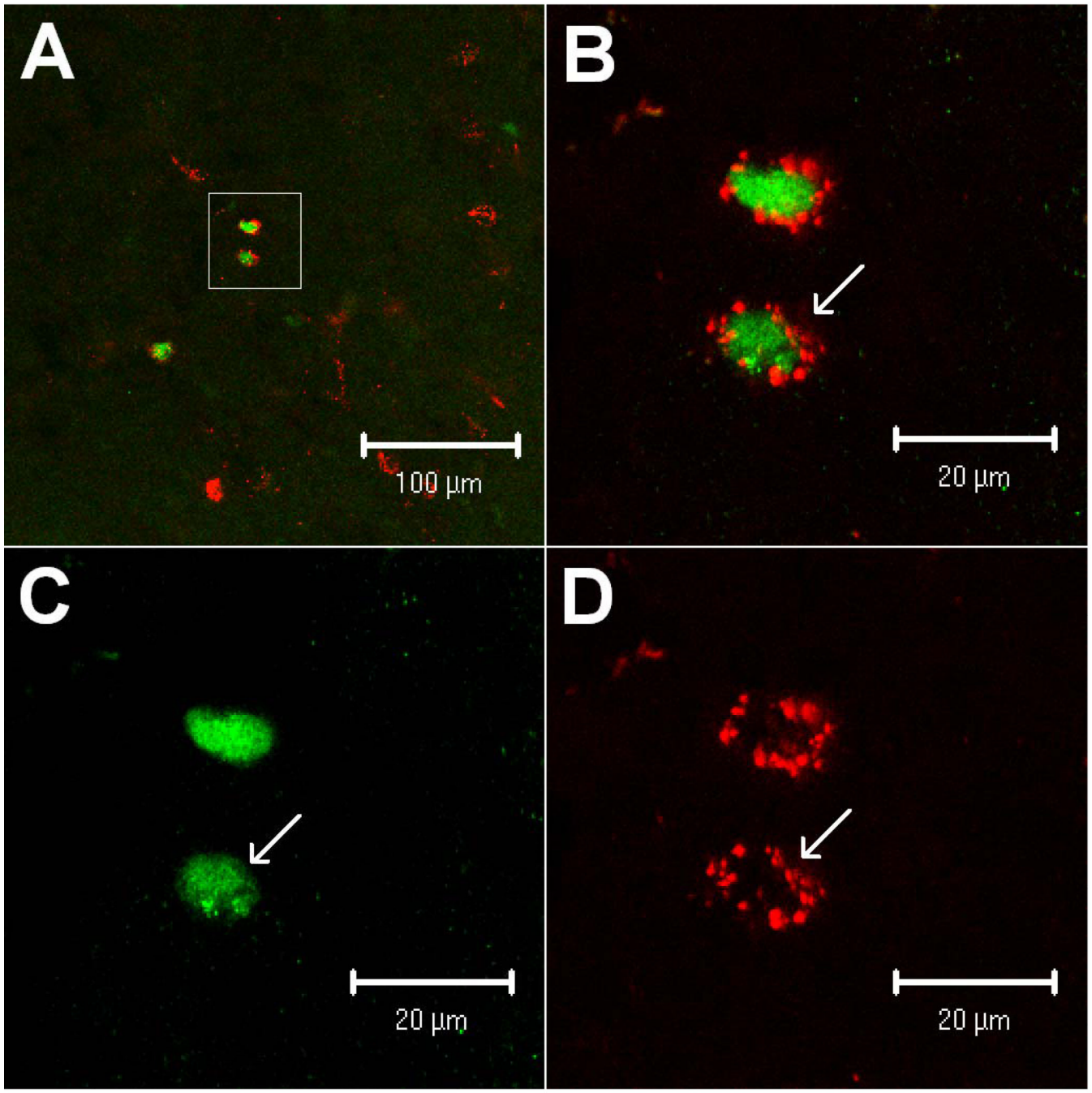

Figure 2.

Confocal microscopic images of neurons double-labeled with a retrograde microsphere tracer injected into the ventrolateral periaqueductal gray and c-Fos in the arcuate nucleus (Bregma −2.04 mm) of a rat following electroacupuncture. A: low-power photomicrograph. B: magnified region shown within the box in A. B is a merged image from C and D. Arrows in B–D indicate a neuron co-labeled with c-Fos and the retrograde microsphere tracer, Fos positive nucleus and retrograde microsphere tracer, respectively. Scale bars in A, B–D represent 100 and 20 µm, correspondingly.

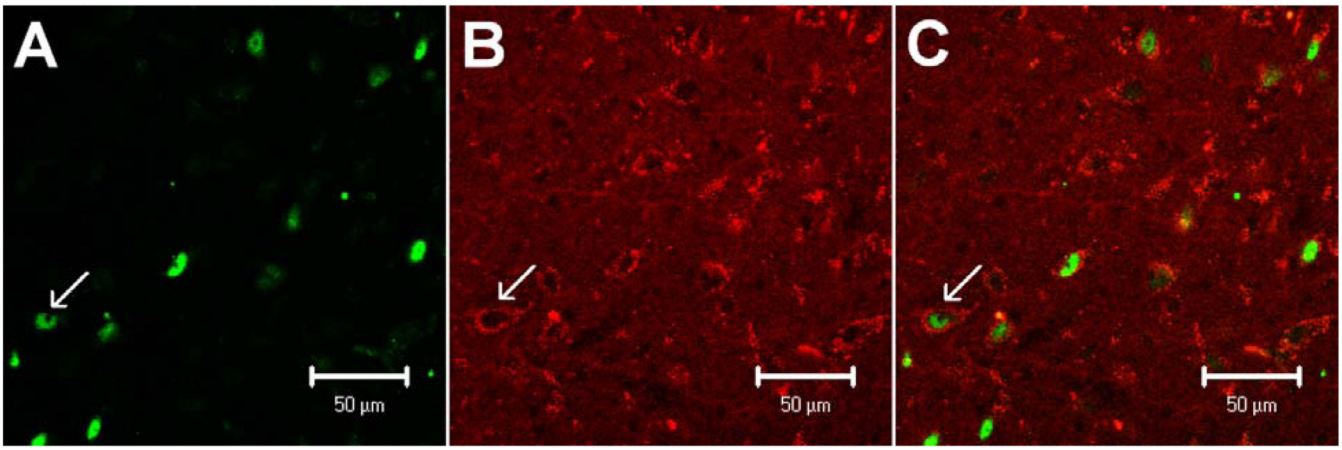

Figure 3.

Confocal microscopic images showing neurons double-labeled with the retrograde microsphere tracer injected into the arcuate nucleus and c-Fos in the ventrolateral periaqueductal gray (Bregma −7.92 mm) of a rat following electroacupuncture. C is a merged image from A and B. Arrows in A–C indicate a Fos positive nucleus, a neuron labeled with retrogradely transported microspheres and co-localization of c-Fos immunoreactivity and the retrograde tracer, respectively. Scale bars in A–C represent 50 μm.

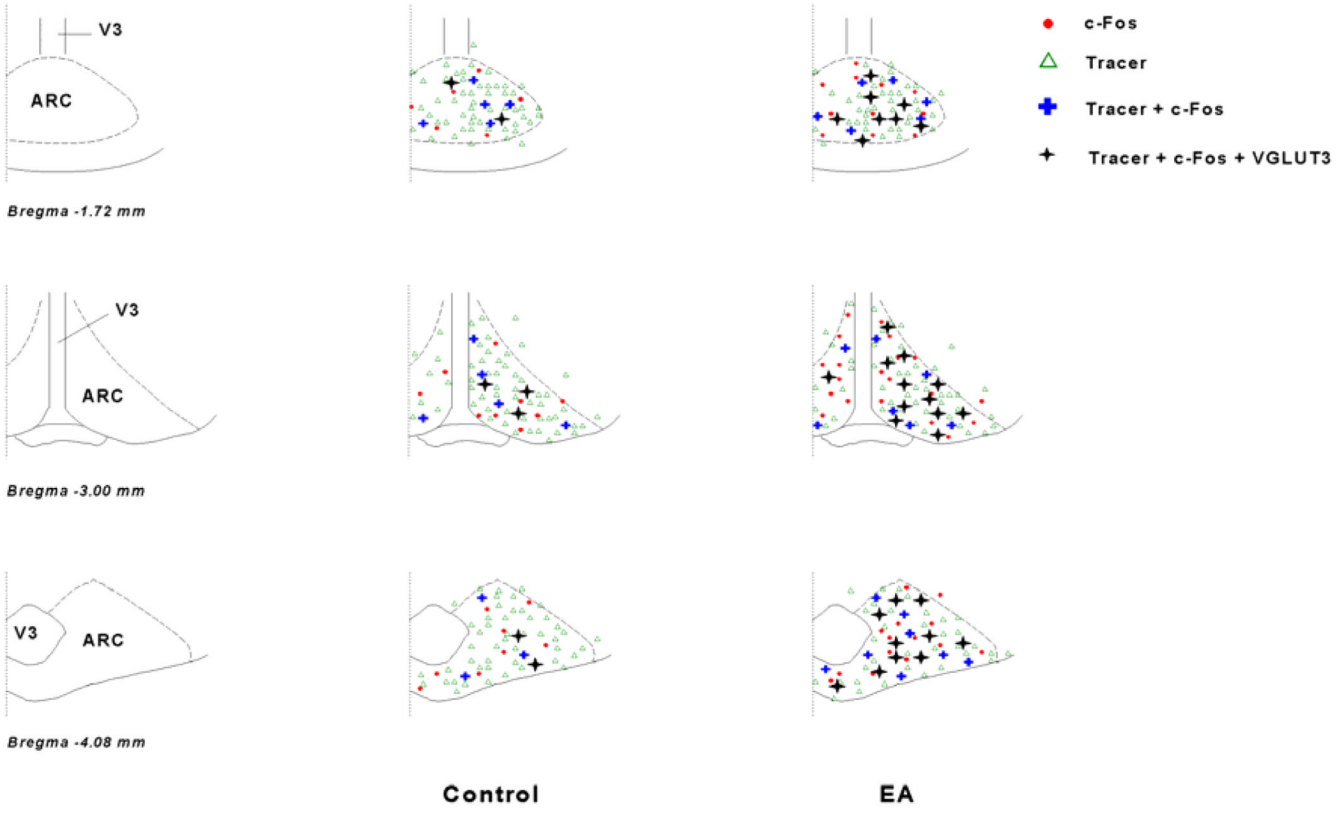

Figure 4.

Distribution of cells labeled with retrograde microsphere tracer (tracer) and/or c-Fos immunoreactivity, and co-localization with vesicular glutamate transporter 3 (VGLUT3) in the arcuate nucleus (ARC) following electroacupuncture (EA) and in a sham-operated control. Three ipsilateral coronal sections to the injected site of the tracer (Paxinos and Watson's atlas) were selected from one animal in each experimental group. Each symbol represents one labeled cell with c-Fos, tracer, c-Fos + tracer or c-Fos + tracer +VGLUT3, respectively. V3, third ventricle.

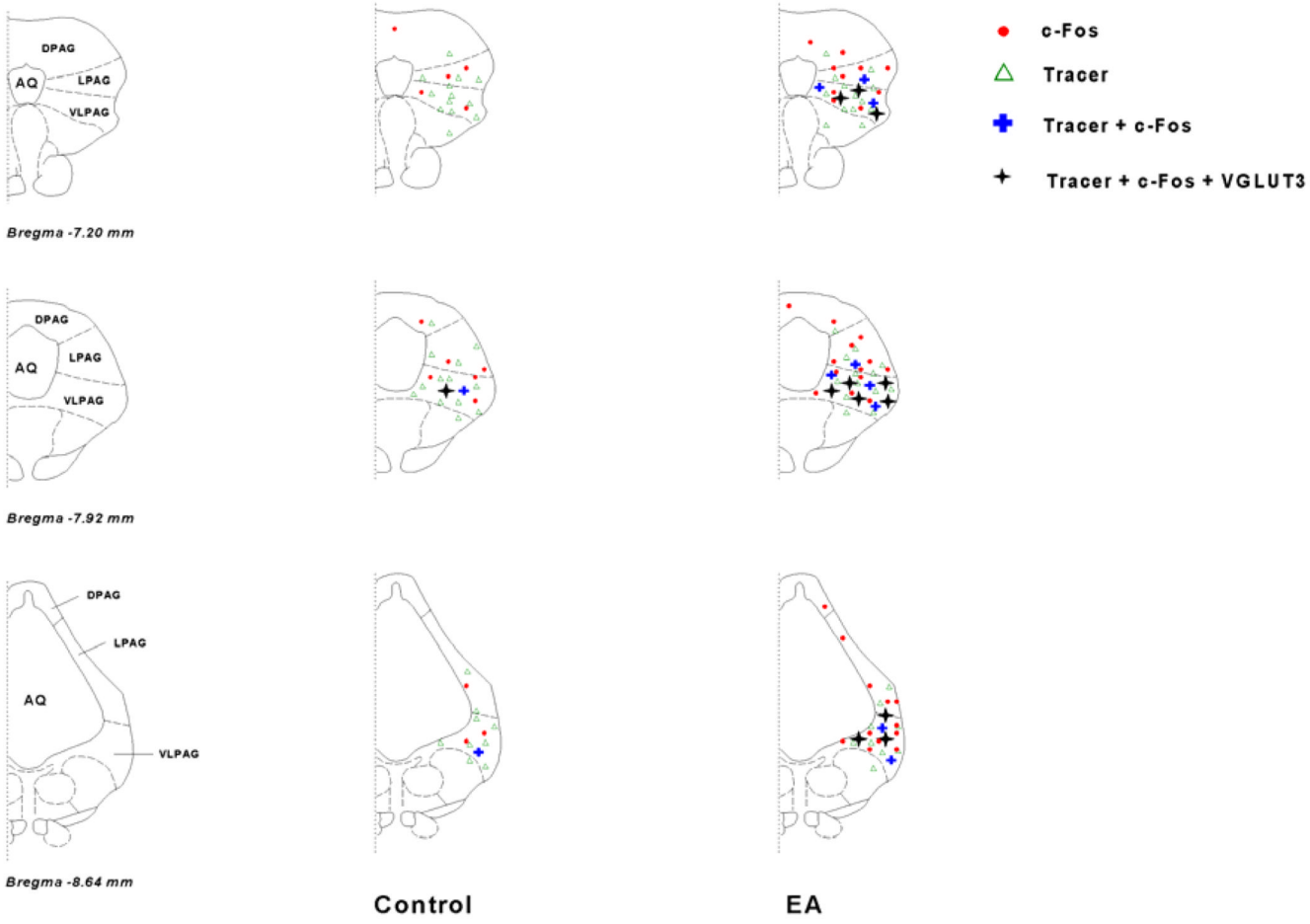

Figure 5.

Distribution of cells labeled with retrograde microsphere tracer (tracer) and/or c-Fos immunoreactivity, and co-localization with vesicular glutamate transporter 3 (VGLUT3) in the ventrolateral periaqueductal gray (VLPAG) following electroacupuncture (EA) and in a sham-operated control. Three ipsilateral coronal sections on the injected site of the tracer (Paxinos and Watson's atlas) were selected from one animal in each experimental group. Each symbol represents labeled cells: Δ, ten cells labeled with the tracer; •, two c-Fos positive nuclei; +, five neurons co-labeled with c-Fos + tracer; *, two cells triple-labeled with c-Fos + tracer +VGLUT3. AQ, aqueduct; DPAG, dorsal periaqueductal gray; LPAG, lateral periaqueductal gray.

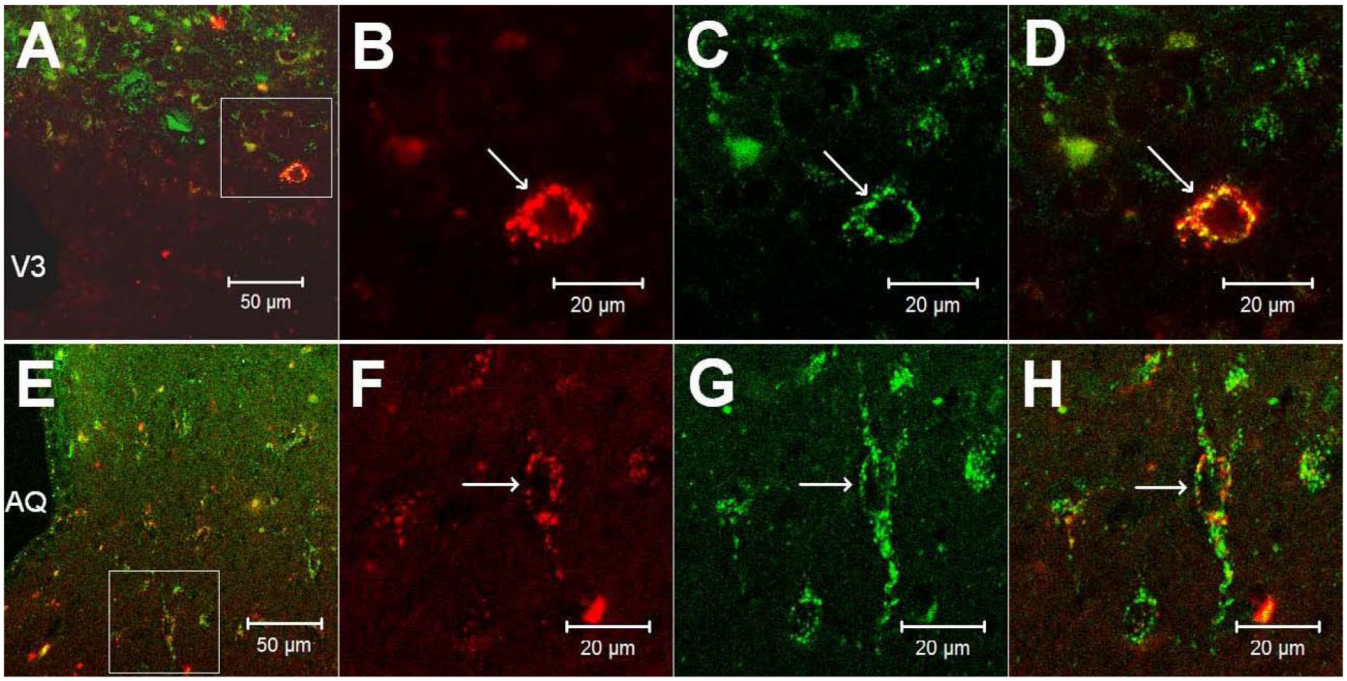

Figure 6.

Confocal microscopic images showing neurons double-labeled with vesicular glutamate transporter 3 (VGLUT3) and retrograde microsphere tracer (tracer) in the brain sections of rats. Panels A–D and E–H depict labeled neurons in the arcuate nucleus (ARC; Bregma −3.24 mm) and ventrolateral periaqueductal gray (vlPAG; Bregma −8.52 mm) after microinjection of the tracer into the vlPAG and ARC, respectively. A and E: low-power photomicrographs; B and F: magnified regions shown within box in A and E. Panels B and F demonstrate merged images from Panels C – D, and G – H, respectively. Arrows in Panels C and G, D and H, and B and F indicate neurons containing the tracer (red), $VGLUT_3$ (green) and two labels, respectively. Scale bars in panels A, E, and B–D and F–H represent 200, 100, and 50 μm, respectively. V3, third ventricle; AQ, aqueduct.

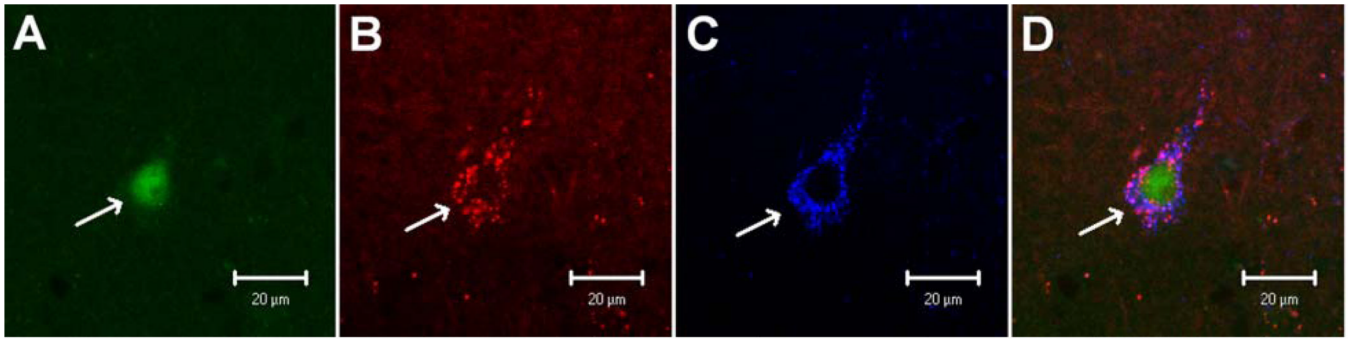

Figure 7.

Confocal microscopic images showing vesicular glutamate transporter 3 (VGLUT3) and the retrograde microsphere tracer that had been injected earlier into the ventrolateral periaqueductal gray and c-Fos in the arcuate nucleus (Bregma −1.72 mm) of a rat treated with electroacupuncture. Panel D displays merged images from Panels A–C. Arrows in Panels A–D indicate a neuron containing c-Fos, tracer, VGLUT3, and c-Fos + tracer + VGLUT3, respectively. Scale bar = 20 μm.

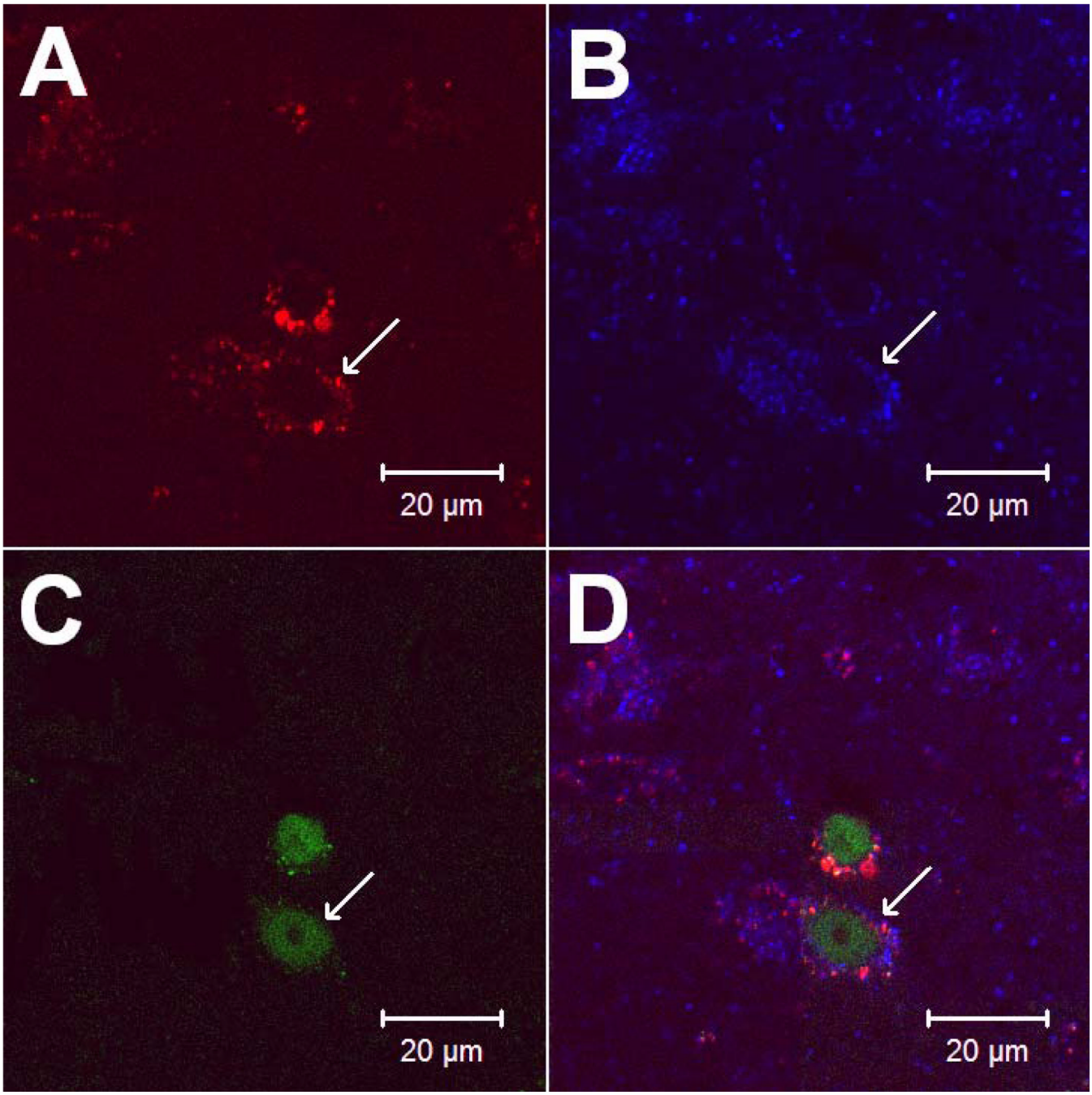

Figure 8.
Confocal microscopic images demonstrating c-Fos, retrograde microsphere tracer (tracer) that had been injected earlier into the arcuate nucleus and vesicular glutamate transporter 3 (VGLUT3) in the ventrolateral periaqueductal gray (Bregma −8.40 mm) of a rat treated with electroacupuncture. Panel D is merged image from Panels A–C. Arrows in Panels A–D indicate a neuron containing the tracer, VGLUT3, c-Fos and c-Fos + tracer + VGLUT3, respectively. Scale bars represent 20 μm.

Table 1

Co-localization of c-Fos with retrograde tracer or retrograde tracer and VGLUT3 in the ARC following electroacupuncture

	Treatment	
	Control (n=5)	**EA (n=6)**
Tracer (no.)	48 ± 7	50 ± 5
Fos (no.)	9 ± 2	29 ± 4*
VGLUT3 (no.)	93 ± 12	102 ± 7
Tracer + Fos (no.)	6 ± 2	16 ± 2*
Tracer + Fos+ VGLUT3 (no.)	3 ± 1	11 ± 2*
(Tracer + Fos)/Fos (%)	68 ± 2	60 ± 8
(Tracer + Fos)/Tracer (%)	12 ± 2	32 ± 3*
(Tracer + Fos+ VGLUT3)/(Tracer + Fos) (%)	45 ± 3	68 ± 5*
Tracer + VGLUT3 (no.)	38 ± 5	39 ± 3
(Tracer + VGLUT3)/Tracer (%)	82 ± 7	79 ± 4
(Tracer + VGLUT3)/VGLUT3 (%)	44 ± 8	39 ± 4
(Tracer + Fos+ VGLUT3)/(Tracer + VGLUT3) (%)	7 ± 2	28 ± 2*

Note: * P< 0.01, EA-treated group versus control group. EA, electroacupuncture; VGLUT3, vesicular glutamate transporter 3; ARC, arcuate nucleus; Tracer, retrograde microsphere tracer.

Table 2

Co-localization of c-Fos with retrograde tracer or retrograde tracer and VGLUT3 in the vlPAG following electroacupuncture

	Treatment	
	Control (n=4)	**EA (n=6)**
Tracer (no.)	77 ± 4	76 ± 4
Fos (no.)	6 ± 1	24 ± 3**
VGLUT3 (no.)	66 ± 2	70 ± 3
Tracer + Fos (no.)	3 ± 1	15 ± 2**
Tracer + Fos+ VGLUT3 (no.)	1 ± 1	8 ± 1**
(Tracer + Fos)/Fos (%)	43 ± 5	63 ± 5*
(Tracer + Fos)/Tracer (%)	4 ± 1	19 ± 3**
(Tracer + Fos+ VGLUT3)/(Tracer + Fos) (%)	40 ± 9	56 ± 8
Tracer + VGLUT3 (no.)	51 ± 6	48 ± 3
(Tracer + VGLUT3)/Tracer (%)	66 ± 6	64± 2
(Tracer + VGLUT3)/VGLUT3 (%)	78 ± 9	70 ± 5
(Tracer + Fos+ VGLUT3)/(Tracer + VGLUT3) (%)	2 ± 1	17 ± 3**

Note: * P< 0.05

** P< 0.01, EA-treated group versus control group. EA, electroacupuncture; VGLUT3, vesicular glutamate transporter 3; vlPAG, ventrolateral periaqueductal gray; Tracer, retrograde microsphere tracer.